Network-based Transcript Quantification with RNA-Seq Data

Wei Zhang [1], Kay Minn [2], Lilong Lin [3], Baolin Wu [4], Jeremy Chien [2], Hui Zheng [3], and Rui Kuang [1,*]

[1]Department of Computer Science and Engineering, University of Minnesota Twin Cities, Minneapolis, MN 55455, USA, [2]Department of Cancer Biology, University of Kansas Medical Center, Kansas City, KS 66160, USA, [3]Key Laboratory of Regenerative Biology, South China Institute for Stem Cell Biology and Regenerative Medicine, Guangzhou Institutes of Biomedicine and Health, Chinese Academy of Sciences, Guangzhou 510530, China and [4]Division of Biostatistics, School of Public Health, University of Minnesota Twin Cities, Minneapolis, MN 55455, USA

arXiv:1403.5029v1 [cs.CE] 20 Mar 2014

ABSTRACT

High-throughput mRNA sequencing (RNA-Seq) provides valuable information for accurate transcript quantification. In this paper, we introduce a Network-based method for RNA-Seq-based Transcript Quantification (Net-RSTQ) to integrate protein domain-domain interaction information with short read alignment for transcript abundance estimation. Based on the observation that the abundances of the neighboring transcripts by domain-domain interactions in the network are positively correlated, Net-RSTQ models the expression of the neighboring transcripts as Dirichlet priors on the likelihood of the observed read alignments against the transcripts in one gene. The transcript abundances of all the genes are then jointly estimated with a heuristic alternating optimization algorithm. We demonstrate in the experiments that (1) qRT-PCR confirmed that Net-RSTQ achieves better transcript quantification accuracy with RNA-Seq data from a stem cell line and an ovarian cancer cell line compared with the models without using transcript network; and (2) the transcript abundances estimated by Net-RSTQ are more informative for patient sample classification tested on the RNA-Seq data of ovarian cancer, breast cancer and lung cancer in The Cancer Genome Atlas (TCGA).

INTRODUCTION

Application of next generation sequencing technologies to mRNA sequencing (RNA-Seq) is becoming a major approach to transcriptome study (1, 2, 3, 4). Compared with microarray technologies, RNA-Seq provides information for expression analysis at transcript level and yet avoids the limitations of cross-hybridization and restricted range of the measured expression levels. Thus, RNA-Seq is particularly useful for quantification of transcript expressions and identification of novel transcripts. Accurate RNA-Seq-based transcript quantification is a crucial step in other downstream transcriptome analyses such as transcript function prediction (5), and differential gene expression analysis (6) or transcript expression analysis (7). Detecting biomarkers from transcript quantifications by RNA-Seq is also a frequent common practices in biomedical research. However, transcript quantification is challenging since a variety of systematical sampling biases have been observed in RNA-Seq data as a result of library preparation protocols (8, 9, 10, 11). Moreover, in the aligned RNA-Seq short reads, most reads mapped to a gene are potentially originated by more than one transcript. The ambiguous mapping could result in hardly identifiable patterns of transcript variants (11, 12).

A useful prior knowledge that has been largely ignored in RNA-Seq transcriptome quantification is the relation among the transcripts by the interactions between their protein products. The protein products of different transcripts coded by the same gene may contain different domains interacting with the protein products of the transcripts in other genes. Thus, the abundance of a transcript in a gene can significantly impact the quantification of the transcripts in other genes when their protein products interact with each other to accomplish a common function as illustrated by a simulated example in Figure S1 in **Supplementary** and a real subnetwork in Figure 1. Motivated by our observation that the protein products of highly co-expressed transcripts are more likely to interact with each other by protein domain-domain binding in four TCGA RNA-Seq datasets (see Figure 3), we constructed a human transcript interaction network based on protein domain-domain interactions to improve transcript quantification. Based on the constructed transcript network, we propose a network-based transcript quantification model called Net-RSTQ to explore domain-domain interaction information for estimating transcript abundance. In the Net-RSTQ model, Dirichlet prior representing prior information in the transcript interaction network is introduced into the likelihood function of observing the short read alignments. The new likelihood function of Net-RSTQ can be alternatively optimized over each gene with expectation maximization (EM) combined with a heuristic search method.

In the experiments, Net-RSTQ was first tested on two cell line RNA-Seq datasets, one of which is the H9 stem cell line and the other is OVCAR8 ovarian cancer cell line. Transcript

*To whom correspondence should be addressed. Tel: +1 612 6247820; Fax: +1 612 6250572; Email: kuang@cs.umn.edu

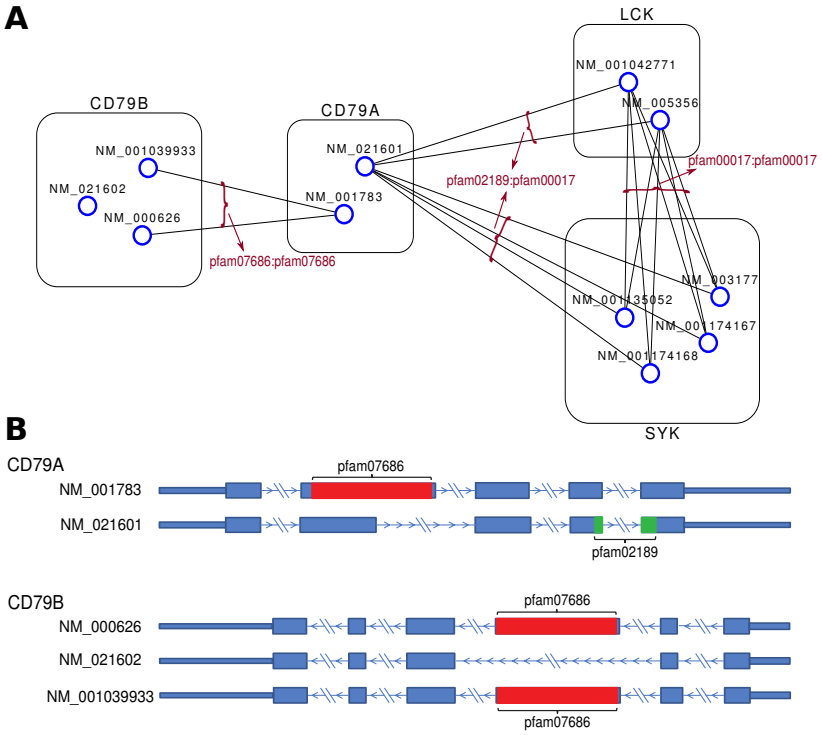

Figure 1. A transcript network based on protein domain-domain interactions. (A) The subnetwork shows the domain-domain interactions among transcripts from four human genes, CD79B, CD79A, LCK and SYK. In the network, the nodes represent transcripts, which are further grouped and annotated by their gene name; and the edges represent domain-domain interactions between two transcripts. Each edge is also annotated by the interacting domains in the two transcripts. (B) RefSeq transcript annotations of CD79A and CD79B are shown with Pfam domain marked in color. The Pfam domains were detected with Pfam-Scan software. Note that no interaction is included between transcripts NM_001039933 and NM_000626 of gene CD79B since self-interactions are not assumed for modeling simplicity (see section **Transcript network construction**). For better visualization, only the interactions coincide with PPI are shown in the figure.

expressions quantified by qRT-PCR were used as ground truth for evaluation. Net-RSTQ was then applied to four cancer RNA-Seq datasets from The Cancer Genome Atlas (TCGA) to quantify transcript expressions in cancer genes of each patient sample. The estimated transcript expressions were used to classify patient samples by the survival or relapse outcomes. Promising results were observed in both experiments.

MATERIALS AND METHODS

In this section, we first describe the construction of the transcript interaction network and review the base probabilistic model for transcript quantification with RNA-Seq data. We then introduce the network-based transcript quantification model (Net-RSTQ) by applying the protein domain-domain interaction information as prior knowledge. The notations used in the equations are summarized in Table 1.

Notation	Description
N	total # of genes
$\boldsymbol{T}$	set of transcripts; T_{ik} is the k^{th} transcript of the i^{th} gene; $\boldsymbol{T}_i$ denotes the transcripts of the i^{th} gene
l_{ik}	length of transcript T_{ik}
$\boldsymbol{r}$	set of reads; r_{ij} is the j^{th} read aligned to the i^{th} gene; $\boldsymbol{r}_i$ is the read aligned to the i^{th} gene
P_{ik}	the probability of a read generated by transcript T_{ik} in the i^{th} gene
$\boldsymbol{\pi}$	transcript expression; π_{ik} is the expression of the k^{th} transcript of the i^{th} gene
ϕ_{ik}	sum of (normalized) expressions of transcript T_{ik}'s neighbors in the transcript network
$\boldsymbol{\alpha}$	Dirichlet prior; $\alpha_{ik} = \lambda\phi_{ik} + 1$ is the Dirichlet prior of T_{ik}
$\boldsymbol{q}_i$	indicator matrix, $q_{ijk} = 1$ if read r_{ij} is aligned to transcript T_{ik}, otherwise $q_{ijk} = 0$
$\boldsymbol{S}$	binary matrix for transcript interaction network

Table 1. Notations

Transcript network construction

A binary transcript network was constructed by measuring the protein domain-domain interactions (DDI) between the domains in each pair of transcripts in four steps. First, the translated transcript sequences of all of human genes were obtained from RefSeq (13). Second, Pfam-Scan was used to search Pfam databases for the matched Pfam domains on each transcript with 1e-5 e-value cutoff (14). Note that only high quality, manually curated Pfam-A entries in the database were used in the search. Third, domain-domain interactions were obtained from several domain-domain interaction databases, and if any domain-domain interaction exists between a pair of transcripts, the two transcripts are connected in the transcript network. Specifically, 6634 interactions between 4346 Pfam domain families from two 3D structure-based DDI datasets (iPfam(15) and 3did (16)) inferred from the protein structures in Protein Data Bank (PDB) (17) were used in the experiments. Besides these highly confident structure-based DDIs, transcript interactions constructed from 2989 predicted high-confidence DDIs and 2537 predicted medium-confidence DDIs in DOMINE (18) were also included if the transcript interaction agrees with protein-protein interactions (PPI) in HPRD (19). In the experiments, we focused on the 898 transcripts from 414 Sanger cancer genes (20). Finally, the transcript network consists of 11736 interactions constructed from the 3D structure-based DDIs and 421 interactions constructed from the predicted DDIs among the 898 transcripts. Note that self-interactions (interactions between transcript(s) in the same gene) are not considered since Net-RSTQ only utilizes positive correlation between the expressions of neighboring transcripts in different genes. For

simplicity, Net-RSTQ assumes that self-interactions will not change the transcript quantification of an individual gene in the model.

In Figure 1 a subnetwork of the transcripts in gene CD79A and CD79B with their direct neighbors in the transcript network is shown. The RefSeq transcript annotations of CD79A and CD79B are shown in Figure 1(B). In CD79A transcript NM_001783 contains an extra domain pfam07686 while transcript NM_021601 only contains a shorter hit pfam02189; and in CD79B transcripts NM_001039933 and NM_000626 contain a domain pfam07686, which is removed in alternative splicing in NM_001039933. In the transcript subnetwork shown in Figure 1(A), the transcripts in CD79A or CD79B clearly have different interaction partners in the network.

Base model for transcript quantification

We first consider the methods proposed in (9, 21, 22, 23) as the base model for quantification of the transcripts in a single gene. The probability that a read is generated by transcript T_{ik} in gene i is modeled by a categorical random variable P_{ik}, where $\sum_{k\in \boldsymbol{T}_i} P_{ik}=1$ and $0\le P_{ik}\le 1$. For any gene i, we consider a total likelihood of the $|\boldsymbol{r}_i|$ short reads aligned to one or more transcripts in $\boldsymbol{T}_i$. The probability of obtaining a read r_{ij} from transcript T_{ik}, $Pr(r_{ij}|T_{ik})$, is modeled by an indicator variable in a $|\boldsymbol{r}_i|\times|\boldsymbol{T}_i|$ matrix $\boldsymbol{q}_i$ with $q_{ijk}=1$ if read r_{ij} is aligned to transcript T_{ik}; otherwise, $q_{ijk}=0$. The likelihood function to estimate $\boldsymbol{P}_i$ from the observed read alignments against gene i is

$$\begin{aligned}\mathcal{L}(\boldsymbol{P}_i;\boldsymbol{r}_i)=Pr(\boldsymbol{r}_i|\boldsymbol{T}_i,\boldsymbol{P}_i) &= \prod_{j=1}^{|\boldsymbol{r}_i|} Pr(r_{ij}|\boldsymbol{T}_i,\boldsymbol{P}_i)\\ &= \prod_{j=1}^{|\boldsymbol{r}_i|}\sum_{k=1}^{|\boldsymbol{T}_i|} Pr(T_{ik})Pr(r_{ij}|T_{ik})\\ &= \prod_{j=1}^{|\boldsymbol{r}_i|}\sum_{k=1}^{|\boldsymbol{T}_i|} P_{ik}q_{ijk}. \end{aligned} \quad (1)$$

Typically, expectation maximization (EM) is applied to obtain the optimal $\boldsymbol{P}_i$ with local maximum likelihood. The relative abundance of the transcript T_{ik} in gene i can be derived from

$$\rho_{ik}=\frac{\frac{P_{ik}}{l_{ik}}}{\sum_{k\in\boldsymbol{T}_i}\frac{P_{ik}}{l_{ik}}}, \quad (2)$$

and the transcript expressions in gene i can be calculated by

$$\pi_{ik}=\frac{|r_i|P_{ik}}{l_{ik}}. \quad (3)$$

Note that the base model is applied independently to each individual gene and no relation among the transcripts is considered.

Network-based transcript quantification model

In the Net-RSTQ model, the transcript interaction network $\boldsymbol{S}$ based on protein domain-domain interactions is introduced to calculate a prior for estimating $\boldsymbol{P}$ jointly across all the genes and all the transcripts. The assumption is that each prior $\boldsymbol{\alpha}_{ik}$ is positively correlated with the neighbors' expression ϕ_{ik}, which is the average expression of the transcript T_{ik}'s neighbors in the transcript network $\boldsymbol{S}$. To be used as a Dirichlet prior, ϕ_{ik} can be normalized as a read count by transcript length as follows

$$\phi_{ik}=l_{ik}(\boldsymbol{\pi}'\frac{\boldsymbol{S}_{ik}}{\sum(\boldsymbol{S}_{ik})}), \quad (4)$$

where $\boldsymbol{S}_{ik}$ is a binary vector represents the neighborhood of transcript T_{ik} in transcript network $\boldsymbol{S}$ and $\sum(\boldsymbol{S}_{ik})$ is the size of neighborhood. The calculation of each ϕ_{ik} is illustrated in Figure 2. A Dirichlet prior $\boldsymbol{\alpha}_i$ for $\boldsymbol{P}_i$ is calculated from the ϕ_{ik} as

$$\alpha_{ik}=\lambda\phi_{ik}+1, \quad (5)$$

where $\lambda>0$ is a tuning parameter.

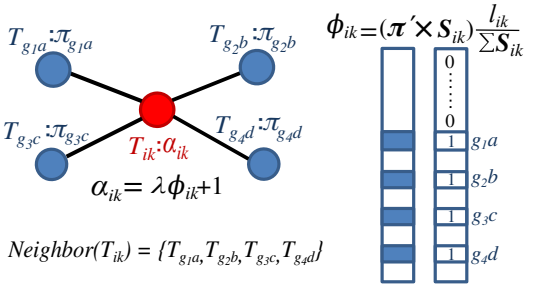

Figure 2. Transcript interaction neighborhood. In this toy example, transcript T_{ik} has four neighbor transcripts $\{T_{g_1a},T_{g_2b},T_{g_3c},T_{g_4d}\}$, which are transcripts from g_1, g_2, g_3 and g_4, respectively. The neighborhood expression ϕ_{ik} of T_{ik} is then calculated as the average of its neighbor transcripts' expressions and further normalized by transcript length, represented as the vector product between $\boldsymbol{\pi}$ and $\boldsymbol{S}_{ik}$ normalized by the number of neighbors $\sum(\boldsymbol{S}_{ik})$ and the transcript length l_{ik} in the figure.

To obtain the optimal $\boldsymbol{P}$ jointly for all genes, we introduce Net-RSTQ model to estimate $\boldsymbol{P}$ iteratively by updating the prior $\boldsymbol{\alpha}$ in each iteration. The new global likelihood function is defined as

$$\mathcal{L}(\boldsymbol{P},\boldsymbol{\alpha};\boldsymbol{r})=\prod_{i=1}^{N}\mathcal{L}(\boldsymbol{P}_i,\boldsymbol{\alpha}_i;\boldsymbol{r}_i)=\prod_{i=1}^{N}Pr(\boldsymbol{P}_i|\boldsymbol{\alpha}_i)Pr(\boldsymbol{r}_i|\boldsymbol{P}_i). \quad (6)$$

Note that the model assumes that the transcript quantification for each gene is still independent when the Dirichlet priors are explicitly modeled. Each prior $Pr(\boldsymbol{P}_i|\boldsymbol{\alpha}_i)$ follows the Dirichlet distribution,

$$Pr(\boldsymbol{P}_i|\boldsymbol{\alpha}_i)=C(\boldsymbol{\alpha}_i)\prod_{k=1}^{|\boldsymbol{T}_i|}P_{ik}{}^{\alpha_{ik}-1}, \quad (7)$$

$$\text{where } C(\boldsymbol{\alpha}_i)=\frac{\Gamma(\sum_k\alpha_{ik})}{\prod_k\Gamma(\alpha_{ik})}.$$

Integrating with equations (**1**) and (**7**), the total likelihood in equation (**6**) can be rewritten as

$$\mathcal{L}(\boldsymbol{P},\boldsymbol{\alpha};\boldsymbol{r})=\prod_{i=1}^{N}\left[C(\boldsymbol{\alpha}_i)\prod_{k=1}^{|\boldsymbol{T}_i|}P_{ik}{}^{\alpha_{ik}-1}\right]\left[\prod_{j=1}^{|\boldsymbol{r}_i|}\sum_{k=1}^{|\boldsymbol{T}_i|}P_{ik}q_{ijk}\right] \quad (8)$$

Replacing the Dirichlet prior $\boldsymbol{\alpha}_i$ with $\alpha_{ik}=\lambda\phi_{ik}+1$ leads to

$$\mathcal{L}(\boldsymbol{P};\boldsymbol{r})=\prod_{i=1}^{N}\left[C(\lambda\boldsymbol{\phi}_i+1)\prod_{k=1}^{|\boldsymbol{T}_i|}P_{ik}{}^{\lambda\phi_{ik}}\right]\left[\prod_{j=1}^{|\boldsymbol{r}_i|}\sum_{k=1}^{|\boldsymbol{T}_i|}P_{ik}q_{ijk}\right] \quad (9)$$

In the likelihood function in equation (**9**), the only hyper-parameter is λ to balance the proportion between the Dirichlet priors and the observed read counts of each transcript. The larger the λ, the more belief put on the priors.

The Net-RSTQ algorithm

The Net-RSTQ algorithm is a heuristic strategy to optimize equation (**9**) by dividing the optimization into sub-optimization problems of sequentially estimating each $\boldsymbol{P}_i$. Specifically, we fix all $\boldsymbol{P}_c$, $c\in\boldsymbol{T}-i$, and thus $\boldsymbol{\phi}_i$ when estimating $\boldsymbol{P}_i$ with EM algorithm (described in the next section) in each iteration and repeat the process multiple rounds throughout all the genes. In each step, the neighborhood expression $\boldsymbol{\phi}$ is recomputed with new $\boldsymbol{P}_i$ for computing the quantification of the next gene. For each sub-optimization problem, we estimate $\boldsymbol{P}_i$ with a fixed $\boldsymbol{\phi}$, the part of the likelihood function in

equation (**9**) involved with the current variables $\boldsymbol{P}_i$ is

$$\bar{\mathcal{L}}(\boldsymbol{P}_i;\boldsymbol{r}_i) = \left[\prod_{g\in \boldsymbol{nb}(i)} C(\lambda\boldsymbol{\phi}g+1)\prod_{k=1}^{|\boldsymbol{T}_g|} P_{gk}{}^{\lambda\phi_{gk}}\right] \left[C(\lambda\boldsymbol{\phi}_i+1)\prod_{k=1}^{|\boldsymbol{T}_i|} P_{ik}{}^{\lambda\phi_{ik}}\right]\left[\prod_{j=1}^{|\boldsymbol{r}_i|}\sum_{k=1}^{|\boldsymbol{T}_i|} P_{ik}q_{ijk}\right] \quad (10)$$

where $\boldsymbol{nb}(i)$ is the set of the genes containing transcripts that are neighbors of the transcripts in gene i in the transcript network. Equation (**10**) consists of three terms separated by the braces. The second and the third terms are the Dirichlet prior and the likelihood of the observed counts in the data for gene i. The first term is the Dirichlet priors of the neighbor transcripts of each T_{ik}. These prior probabilities are involved since $\boldsymbol{\phi}_g$ are functions of the current variable $\boldsymbol{P}_i$ (equations (**3**)-(**5**)). Equation (**10**) cannot be easily solved with standard techniques. We adopt a heuristic approach to only take steps that will increase the complete likelihood function in equation (**9**). The Net-RSTQ algorithm is outlined below

Algorithm 1 NET-RSTQ

1: **Initialization**: random initialization or EM (equation (**1**)) estimation of $\boldsymbol{P}^{(0)}$
2: **for** round $t=1,\ldots$ **do**
3: $\quad\boldsymbol{P}^{(t)}=\boldsymbol{P}^{(t-1)}$
4: $\quad$**for** gene $i=1,\ldots,N$ **do**
5: $\quad\quad$compute $\boldsymbol{\phi}_i$ based on $\boldsymbol{P}^{(t)}$ with equations (**3**) and (**4**)
6: $\quad\quad$estimate $\boldsymbol{P}_i$ with EM algorithm (see next section)
7: $\quad\quad$**if** $\bar{\mathcal{L}}(\boldsymbol{P}_i)>\bar{\mathcal{L}}(\boldsymbol{P}_i^{(t)})$ **then**
8: $\quad\quad\quad\boldsymbol{P}_i^{(t)}=\boldsymbol{P}_i$
9: $\quad\quad$**end if**
10: $\quad$**end for**
11: $\quad$**if** $max(abs(\boldsymbol{P}^{(t)}-\boldsymbol{P}^{(t-1)}))<$1e-6 **then**
12: $\quad\quad$**break**
13: $\quad$**end if**
14: **end for**
15: **return** $\boldsymbol{P}$

In the algorithm, the outer for-loop between line 2-14 performs multiple passes of updating $\boldsymbol{P}$. The inner for-loop between line 4-10 scans through each gene to update each $\boldsymbol{P}_i$. Line 7 checks the the difference in the part likelihood of gene i before and after the estimated $\boldsymbol{P}_i$ is applied. The estimated $\boldsymbol{P}_i$ is kept in line 8 only if the part likelihood $\bar{\mathcal{L}}$ in equation (**10**) is higher. The convergence of $\boldsymbol{P}$ is checked at line 11. In each sub-optimization problem, EM algorithm (described in the next section) is applied to estimate $\boldsymbol{P}_i$. After convergence, the transcripts expression $\boldsymbol{\pi}$ can be learned by equation (**3**) with the optimal $\boldsymbol{P}$.

Estimating $\boldsymbol{P}_i$ given $\boldsymbol{\phi}_i$

In line 6 of Algorithm 1, we maximize the likelihood function of the sub-optimization problem in equation (**10**) to learn $\boldsymbol{P}_i$ as

$$\mathcal{L}(\boldsymbol{P}_i;\boldsymbol{r}_i)=\left[C(\lambda\boldsymbol{\phi}_i+1)\prod_{k=1}^{|\boldsymbol{T}_i|} P_{ik}{}^{\lambda\phi_{ik}}\right]\left[\prod_{j=1}^{|\boldsymbol{r}_i|}\sum_{k=1}^{|\boldsymbol{T}_i|} P_{ik}q_{ijk}\right] \quad (11)$$

Note that equation (**11**) is the part of equation (**10**) ignoring the Dirichlet priors of the neighboring genes. In line 7 of Algorithm 1, the ignored Dirichlet priors are combined with the likelihood in equation (**11**), when $\bar{\mathcal{L}}(\boldsymbol{P}_i)$ is computed, to evaluate the whole likelihood in equation (**10**). The likelihood function in equation (**11**) is defined on a categorical variable with Dirichlet prior, which can be solved with EM. By EM formulation, the expectation a_{ijk}, a soft assignment of read j to transcript k in gene i, is first estimated in the expectation step and $\boldsymbol{P}_i$ is then learned in the maximization step. When $\boldsymbol{\phi}_i$ is given, by taking log of equation (**11**) we can write the EM steps to find $\boldsymbol{P}_i$ below.

E step:

Letting ***Match*** signify a matching between reads and transcripts, and *Match(j)* be the transcript from which read j originates, we get:

$$\log[\mathcal{L}(\boldsymbol{P}_i;\boldsymbol{r}_i,\boldsymbol{Match})] = \log C(\lambda\boldsymbol{\phi}_i+1)+\sum_{k=1}^{|\boldsymbol{T}_i|}\lambda\phi_{ik}\log(P_{ik}) + \sum_{j=1}^{|\boldsymbol{r}_i|}\log(P_{iMatch(j)}q_{ijMatch(j)}) \quad (12)$$

which leads to

$$\begin{aligned} Q(\boldsymbol{P}_i|\boldsymbol{P}_i^{(it)}) &= E_{\boldsymbol{Match}|\boldsymbol{r}_i,\boldsymbol{P}_i^{(it)}}[\log(\mathcal{L}(\boldsymbol{P}_i;\boldsymbol{r}_i))] \\ &= \log C(\lambda\boldsymbol{\phi}_i+1)+\sum_{k=1}^{|\boldsymbol{T}_i|}\lambda\phi_{ik}\log(P_{ik}) \\ &+ \sum_{j=1}^{|\boldsymbol{r}_i|}\sum_{k=1}^{|\boldsymbol{T}_i|}(\log P_{ik}+\log q_{ijk})*\frac{P_{ik}^{(it)}q_{ijk}}{\sum_{k=1}^{|\boldsymbol{T}_i|}P_{ik}^{(it)}q_{ijk}} \\ &= \log C(\lambda\boldsymbol{\phi}_i+1)+\sum_{k=1}^{|\boldsymbol{T}_i|}\lambda\phi_{ik}\log(P_{ik}) \\ &+ \sum_{j=1}^{|\boldsymbol{r}_i|}\sum_{k=1}^{|\boldsymbol{T}_i|}a_{ijk}\log(P_{ik}) \\ &+ \sum_{j=1}^{|\boldsymbol{r}_i|}\sum_{k=1}^{|\boldsymbol{T}_i|}a_{ijk}\log(q_{ijk}) \end{aligned} \quad (13)$$

where it is the it^{th} iteration in EM and

$$a_{ijk}=\frac{P_{ik}^{(it)}q_{ijk}}{\sum_{k=1}^{|\boldsymbol{T}_i|}P_{ik}^{(it)}q_{ijk}}. \quad (14)$$

M step:

Given that q_{ijk} and $\boldsymbol{\phi}_i$ are fixed, the above reduces to maximizing

$$(\boldsymbol{P}_i^{(it+1)})=\arg\max_{\boldsymbol{P}_i}\left[\sum_{k=1}^{|\boldsymbol{T}_i|}\lambda\phi_{ik}log(P_{ik})+\sum_{j=1}^{|\boldsymbol{r}_i|}\sum_{k=1}^{|\boldsymbol{T}_i|}a_{ijk}log(P_{ik})\right] \quad (15)$$

Using Lagrange multipliers and differentiating, equation (**15**) is maximized when

$$P_{ik}^{(it+1)}=\frac{\lambda\phi_{ik}+\sum_{j=1}^{|\boldsymbol{r}_i|}a_{ijk}}{\sum_{k=1}^{|\boldsymbol{T}_i|}(\lambda\phi_{ik}+\sum_{j=1}^{|\boldsymbol{r}_i|}a_{ijk})}. \quad (16)$$

After EM algorithm converge, we update $\boldsymbol{P}$ with the new estimated $\boldsymbol{P}_i$ only if lead to a increasing equation (**10**).

RESULTS

In the experiments, Net-RSTQ was applied to estimate RNA transcript expression for two cell line datasets and four TCGA cancer datasets. We first demonstrate that in the TCGA cancer datasets transcript co-expression strongly correlates with protein domain-domain interactions to motivate modeling with Net-RSTQ. Net-RSTQ was compared with EM (the base

model in equation (**1**)), Cufflinks (4) and RSEM (transcript expression or gene expression) (24). We measured accuracy of transcript quantification evaluated by qRT-PCR on the two cell lines and cancer outcome prediction based on the estimated transcript/gene expressions on four cancer datasets. Statistical assessment was also performed on randomized transcript networks to evaluate the significance of the results by Net-RSTQ.

RNA-Seq data preparation

Two cell line RNA-Seq datasets were used for evaluating the accuracy of transcript quantification by comparison with qRT-PCR. The first dataset is the H9 embryonic stem cell line data from (25). The raw RNA-Seq fastq file were downloaded from SRA website (SRR1015682) under GEO accession GSE51607. The other dataset is from the OVCAR8 ovarian cancer cell line. The raw fastq file was prepared at University of Kansas Medical Center. There were 23,397,325 single-end 34bp reads in the stem cell line dataset and 19,892,473 paired-end 100bp reads in the OVCAR8 mapped to the human hg19 reference genome by TopHat (26) with up to 2 mismatches allowed. Exon coverages and read counts of exon-exon junctions were generated by SAMtools (27) to be utilized with Net-RSTQ and EM (equation (**1**)). Cufflinks (4) directly infers transcript expressions based on the alignment by TopHat. The above cell line data were used to generate the results in Figure 4, Figure 5 and Table S1 and S2 in **Supplementary**.

Cancer Type	Event	# of Patients by years
Ovarian serous cystadenocarcinoma(OV)	Survival	76(<3 ys) **vs** 62(>4 ys)
	Relapse	79(<1.5 ys) **vs** 68(>2 ys)
Breast invasive carcinoma(BRCA)	Survival	66(<5 ys) **vs** 57(>8 ys)
	Relapse	42(<5 ys) **vs** 38(>8 ys)
Lung adenocarcinoma(LUAD)	Survival	47(<2 ys) **vs** 56(>3 ys)
Lung squamous cell carcinoma(LUSC)	Survival	67(<2 ys)**vs** 77 (>3 ys)

Table 2. Summary of patient samples in TCGA datasets. The patients are categorized by cutoffs on survival and relapse time based on the available clinical information in each dataset.

TCGA RNA-Seq datasets of Ovarian serous cystadenocarcinoma (OV), Breast invasive carcinoma (BRCA), Lung adenocarcinoma (LUAD) and Lung squamous cell carcinoma (LUSC) were analyzed for patient outcome prediction with transcript expressions estimated by Net-RSTQ, EM (equation (**1**)) and RSEM (24). The patient samples in each dataset were first classified into cases and controls based on the survival and relapse outcomes as shown in Table 2. The raw read counts were downloaded from TCGA with data type "RNASeqV2" at level 3 mapped to hg19 exon annotations. Both the gene expression and transcript expression data reported by RSEM (24) in TCGA (level 3 data) were utilized as two baselines for cancer outcome prediction in Table 3. In addition, the raw RNA-Seq fastq files (level 1 data) of ovarian cancer were downloaded from Cancer Genomics Hub (CGHub) and processed by TopHat and Cufflinks workflow as another additional baseline for comparison.

In the experiment on both cell line and TCGA datasets, we focused on transcript quantification and cancer outcome prediction with a list of 414 cancer genes from Sanger Institute (20) for better cancer relevance. The NCBI RefSeq annotation (13) were applied to match the transcripts in 414 cancer genes to their transcript isoforms, resulting a transcript network of the 898 transcripts in the 414 cancer genes.

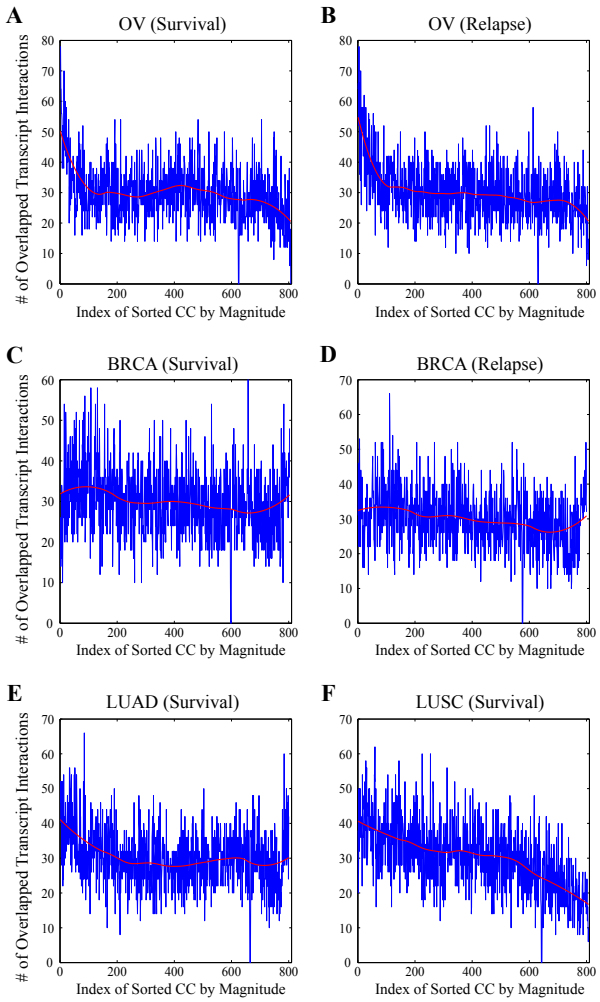

Figure 3. Correlation between transcript co-expression and protein domain-domain interaction in TCGA datasets. The correlation coefficients between transcript expressions across all patient samples are first calculated in each dataset for each pair of transcripts by EM model (equation (**1**)). The correlation coefficients are then sorted from largest to smallest and grouped into bins of size 1000 each. The x-axis is the index of the bins with lower index indicating larger correlation coefficients. The y-axis is the number of transcript pairs of transcripts in each bin coincide with at least one protein domain-domain interaction between the transcript pair. The red line is the smooth plot by fitting local linear regression method with weighted linear least squares (LOWESS) to the curves.

Transcript co-expressions correlate with protein domain-domain interactions

Without assuming any prior knowledge of protein domain-domain interaction, the EM model in equation (**1**) was used to quantify the transcript expression in the TCGA datasets in Table 2. The transcript co-expressions were then calculated by Pearson's correlation coefficients of each pair of transcripts across all the samples in each dataset. The pairwise correlation coefficients were sorted from the largest to the smallest and grouped into bins of size 1000. The number of transcript

pairs with protein domain-domain interaction in the transcript network are reported in Figure 3. In the OV, LUAD and LUSC datasets, there is a clear trend that highly co-expressed transcripts are more likely to interact with each other in the transcript network. The signal in the breast cancer datasets is less prominent although the difference is distinguishable in the LOWESS fitting. The observations support that protein domain-domain interactions provide additional information for quantifying co-expressed transcripts. Note that in the right end of the plots, the protein products of negatively correlated transcripts may also have a slightly higher chance to interact with each other. We observed that the protein products of transcript are often involved in kinase activities, which might be negative gene regulation related to post-translational regulation. Since both the number and the magnitude of negatively correlated transcript pairs are much less, we observed that the contribution to the transcript quantification and classification is minimal in our experiments when the interactions with negative correlations were removed (Table S3 in **Supplementary**).

qRT-PCR confirms improved transcript quantification by Net-RSTQ

To evaluate the accuracy of transcript quantification, the transcript abundance estimated by Net-RSTQ, EM (equation (**1**)), and Cufflinks are compared to the qRT-PCR results on the two cell lines. Parameter $\lambda = 0.1$ was fixed in the Net-RSTQ experiments. Among the genes that Net-RSTQ and EM report most different quantification results, qRT-PCR experiments were performed to test the genes with relatively high coverage, two to three transcripts, and availability of the primer designs to distinguish the transcripts in the qRT-PCR products (see Table S4 and S5). The selection left seven genes to be tested in H9 stem cell line and five genes in OVCAR8 ovarian cancer cell line. Three replicates of H9 stem cell line and two replicates of OVCAR8 cell line were tested.

The relative abundance of the seven genes in H9 stem cell line are shown in Figure 4(A) and Table S1. The qRT-PCR results were generated by three replicates and the standard deviations are also plotted. More details of the qRT-PCR experiment design can be found in **Supplementary**. In all the seven genes, the relative abundance estimated by Net-RSTQ are closer to the qRT-PCR results compare to the results by EM and Cufflinks. To directly measure the difference in performance between Net-RSTQ and EM and between Net-RSTQ and Cufflinks, a scatter plot of the Kullback-Leibler divergence (28) to the qRT-PCR results between two methods are shown in Figure 5(A). In the scatter plot, the estimated relative abundances by Net-RSTQ are much closer to qRT-PCR results.

The same comparisons on the fives selected genes in OVCAR8 ovarian cancer cell line are shown in Figure 4(B) and Table S2. The qRT-PCR results were generated by two replicates. The scatter plots of the Kullback-Leibler divergence to the qRT-PCR results are shown in Figure 5(B). Cufflinks only reports expression of one transcript in four genes, only one of which, agrees with the highly expressed transcript in the qRT-PCR results. Thus, Cufflinks does not perform reasonably well for comparison with Net-RSTQ. Compared with the results by EM, Net-RSTQ performed

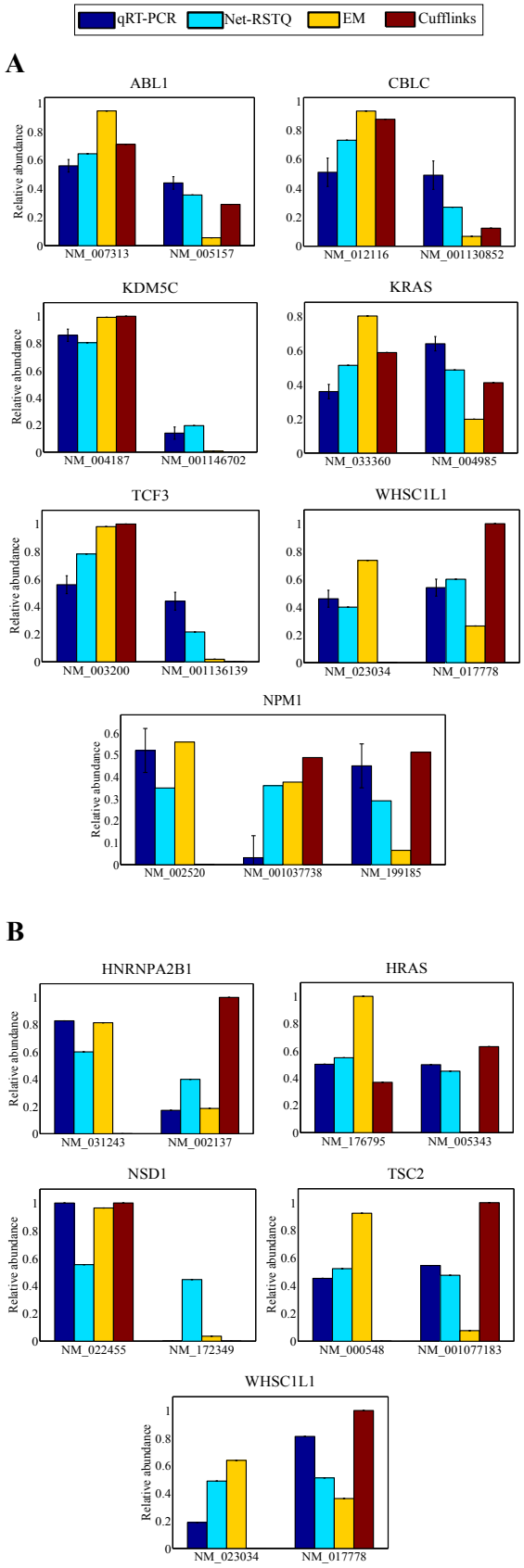

Figure 4. Evaluation by qRT-PCR experiments. The relative abundance of the transcripts in seven genes of H9 stem cell line (A) and five genes of OVCAR8 ovarian cancer cell line (B) estimated by Net-RSTQ, EM and Cufflinks were compared with the qRT-PCR experiments. The total abundance is normalized to 1 over the measured transcripts in each gene.

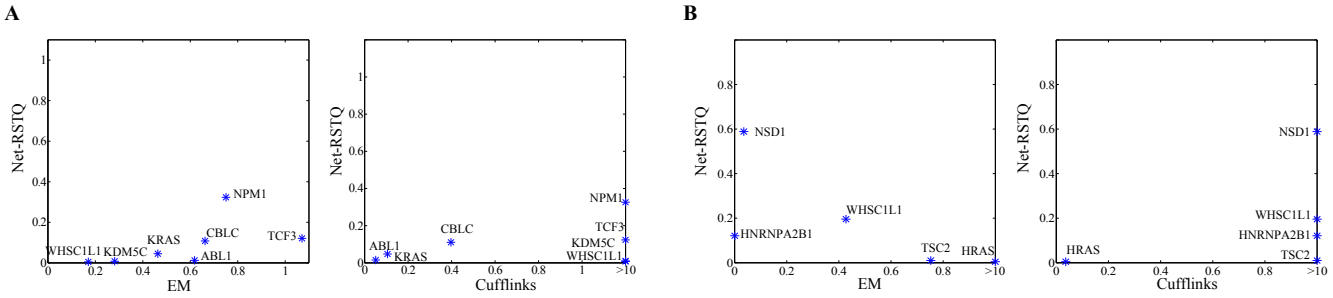

Figure 5. Kullback-Leibler divergence. Kullback-Leibler divergence was applied to evaluate how close the relative abundance estimated by Net-RSTQ, EM, and Cufflinks is to the qRT-PCR results. The smaller the divergence, the closer. (A) Results on H9 stem cell line data and (B) Results on OVCAR8 cancer cell line data are shown by bar plots. Note that when 0 proportion is reported, very small prior is added for calculating KL divergence.

better on three genes and worse on two genes, NSD1 and HNRNPA2B1. Note that Net-RSTQ still correctly identified that the proportion of NM_031243 is higher than NM_002137 in HNRNPA2B1 and that of NM_022455 is higher than NM_172349 in NSD1. It is possible that transcript expression of NM_002137 in gene HNRNPA2B1 and NM_172349 in gene NSD1 were slightly over smoothed by network information in Net-RSTQ with a fixed λ parameter. In the next section, we will show that the smoothness provides better features for classification even though the difference is underestimated in some of the cases. Overall, Net-RSTQ improved transcript quantification in the H9 stem cell data and mixed results with more positive cases than negative cases in the OVCAR8 ovarian cancer cell line data.

Net-RSTQ improves cancer outcome prediction

To evaluate the quality of transcript quantification, we designed a cancer outcome prediction task by the assumption that better transcript quantification always leads to better prediction performance. Net-RSTQ was compared with EM (equation (**1**)) and RSEM (24) by classification with the quantification of 898 transcripts (414 gene for RSEM (gene)) on four cancer dataset. Net-RSTQ was also compared with Cufflinks (4) on ovarian cancer dataset. Each dataset is divided into four folds with two folds for training, one fold for validation (parameter tuning on the classification model), and one fold for test in cross-validation. Classification performance was evaluated with Support Vector Machine (SVM) with RBF kernel (29) as the classifier.

We repeated the four-fold cross-validation 100 times by each method in each dataset and report the average receiver operating characteristic (ROC) score across the 100 repeats in Table 3. The transcript expressions estimated by Net-RSTQ always achieved better average classification results than those by the base EM model. To evaluate the statistical significance of the differences between the ROC scores generated by Net-RSTQ and the EM algorithm in the 100 repeats, in Table 3 we also report the p-values by a binomial test on the number of wins/loses in all the experiments between Net-RSTQ and the base EM algorithm. Three cases were significant with very low p-values about or much less than 0.001 and two cases were significant with p-values just below 0.02 while in the BRCA (survival) case, the p-value is only moderately significant even though the average by Net-RSTQ is higher. Net-RSTQ clearly outperforms the base EM model significantly. Net-RSTQ also outperformed RSEM (transcript or gene) in five cases except the experiment on BRCA (relapse) dataset. Cufflinks(4) was also applied to two experiments OV (survival) and OV (relapse). The classification results on transcript expression data estimated by Cufflinks were worse than Net-RSTQ (0.563 vs 0.597 (survival) and 0.577 vs 0.607 (relapse)). By the observations, Net-RSTQ overall performed the best in the classification tasks. To verify the effect of the interactions with negative correlation in transcript expressions, we applied Net-RSTQ to each dataset with a transcript network containing only the interactions with non-negative correlation in expressions. The same classification setup was applied to the estimated expressions. We compared the classification results in Table S3 in **Supplementary**. It is clearly that the effect of the interactions with negative correlation in classification is negligible and the proportion of interactions with negative correlation is much smaller than the ones with positive correlation.

The λ parameter used for Net-RSTQ was first tuned by the ROC score on the validation set and the optimal λ was applied to compute the ROC score on the test set. The process is repeated for each fold and 100 times. To show the effect of varying the λ on the classification performance in Net-RSTQ, we plotted the average ROC score learned from the validation set across the 100 repeats on BRCA (survival) in Figure 6(A). The optimal λ was 0.1 in this case. There is a clear gradient pattern for the optimal λ suggesting that the transcript network is playing an important role in inferring better transcript quantification. In Figure 6(B), the convergence of Net-RSTQ is also illustrated by each gene update and each iteration throughout all the genes.

Statistical assessments

To understand the role of the transcript network in the transcript expression estimation, we used 100 randomized networks to learn the transcript proportion in each experiment with λ fixed to be 0.1. In each randomization, the edges were shuffled among all the transcripts. For transcript expressions learned by each randomized network, we conducted the same four-fold cross validation to compute the average AUCs among 100 repeats. The boxplot of the AUCs learned with the 100 randomized networks is shown in Figure 7. Compared with the classification results from the true transcript network, the result with randomized networks is always worse. Another important observation is that, the median value of the AUCs

Dataset	OV(Survival)	OV(Relapse)	BRCA(Survival)	BRCA(Relapse)	LUAD(Survival)	LUSC(Survival)
Net-RSTQ(Isoform)	**0.5973**	**0.6070**	**0.6826**	0.5902	**0.6353**	**0.5666**
EM(Isoform)	0.5696	0.5886	0.6727	0.5419	0.5789	0.5496
RSEM(Isoform)	0.5865	0.5501	0.6510	**0.6156**	0.6132	0.5362
RSEM(Gene)	0.5911	0.5804	0.6513	0.5581	0.6151	0.5585
p-value(Net-RSTQ vs EM)	0.0011	0.0198	0.1356	2.248e-5	1.948e-8	0.0167

Table 3. Classification performance of estimated transcript expressions and gene expression. The mean AUC scores of classifying patients by estimated transcript (gene) expression in four-fold cross-validation for each dataset are reported. The best AUCs across the four models are bold.

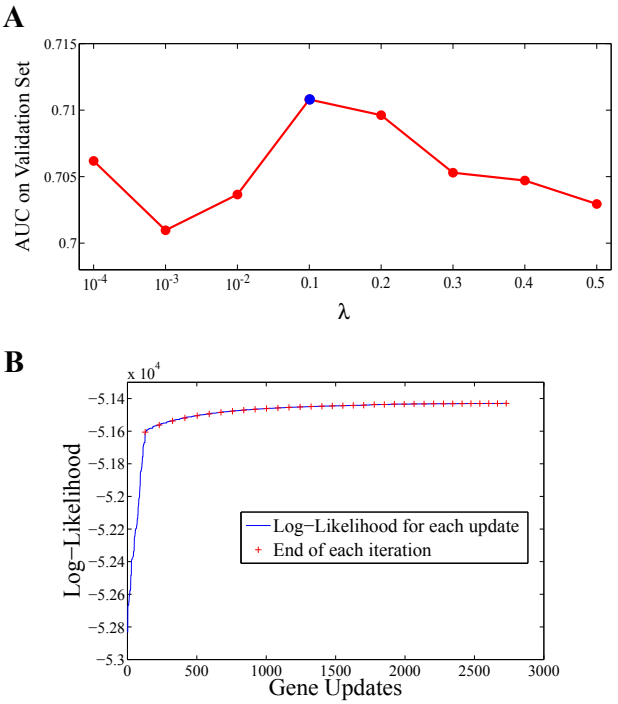

Figure 6. Model selection and convergence. The experiment done on BRCA (survival) dataset. (A) Effect of varying λ on the classification performance. The plot shows the average AUC learned from the 100 repeats on validation set for different λ with the optimal λ in blue. (B) Convergence analysis by the total log-likelihood. The plot shows the change of total log-likelihood in Net-RSTQ with each gene update. Each red cross indicates the end of each round t in line 2 of Algorithm 1.

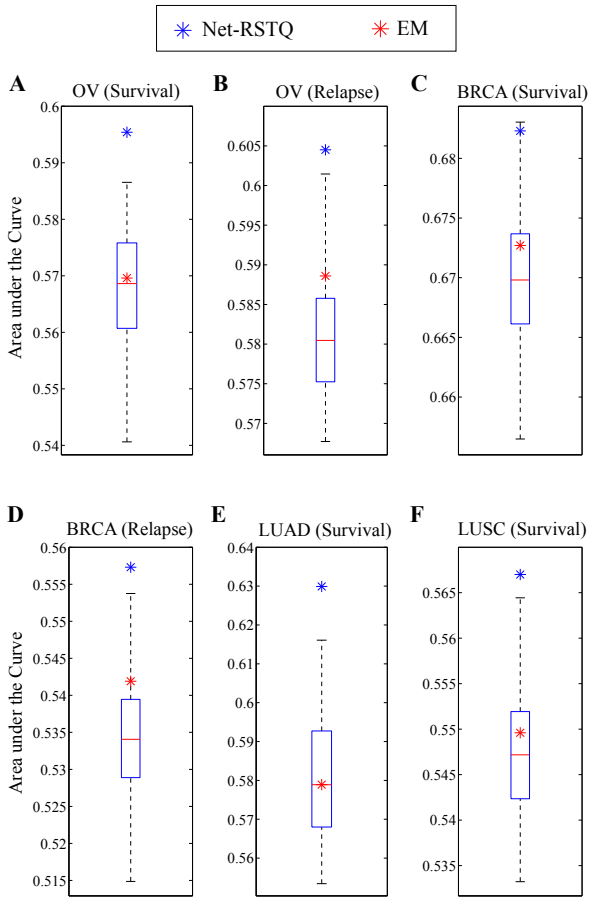

Figure 7. Statistical analysis with randomized networks. Comparison of the classification results by the randomized networks and the true network. The λ parameter was fixed to be 0.1 in all the experiments. The blue star and the red star represent the results with the real network and without network (base EM model), respectively. The boxplot shows the results with the randomized networks.

across the 100 randomized networks is lower or close to the result by the base EM model, which suggests that the randomized networks play no role in improving classification and even lead to worse result. Overall, the results provide a clear evidence that the transcript network is informative for the transcript expression estimation, and supplies more discriminative features for cancer outcome prediction.

Transcript network helps detect novel differentially expressed transcripts

To understand the role of the transcript network in detecting novel differentially expressed transcripts, t-test was applied to the transcript expressions estimated by Net-RSTQ and EM (equation (**1**)) to identify differentially expressed transcripts (p-value$<$0.05). We analyzed the differentially expressed transcripts only identified by Net-RSTQ by examining their neighborhood in the transcript network. Three patterns were observed as illustrated in Figure 8. (1) A transcript in a gene becomes differentially expressed when it is connected to a highly differentially expressed neighbor transcript in another gene. In Figure 8(A), transcript NM_001267706 in gene CD274 is not differentially expressed by EM in the OV (relapse) dataset. However, one of its neighbor NM_001783 in gene CD79A in the transcript network is one of the most differentially expressed transcripts, which smoothes NM_001267706 to be differentially expressed. (2) A transcript becomes differentially expressed when the other peer transcripts are differentially expressed and share the same neighbors with the transcript. In Figure 8(B), three out of the four transcripts except NM_013992 in PAX8 are differentially expressed by EM in the BRCA (survival) dataset. Since all the four transcripts share the same 25 neighbors in the transcript network, NM_013992 was also indirectly

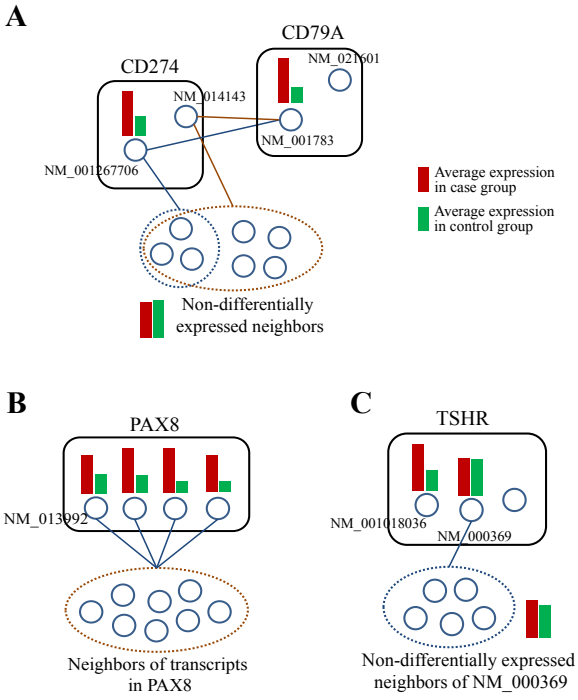

Figure 8. Patterns of novel differentially expressed transcripts. The subnetworks show the three observed patterns of novel differentially expressed transcripts in network-based transcript quantification with Net-RSTQ. (A) Connection with highly differentially expressed neighbor: NM_001267706 is connected to highly differentially expressed NM_001783; (B) Smoothing by other highly differentially expressed peer transcripts in the same gene sharing the same neighbors: NM_013992 is indirectly smoothed by its three differentially expressed peer transcripts in PAX8 since all the four transcripts share the same neighbors; and (C) Proportion changed due to the change of the other peer transcripts in the same gene: NM_001018036 passively becomes differentially expressed because its peer transcript NM_000369 is smoothed by its non-differentially expressed neighbors.

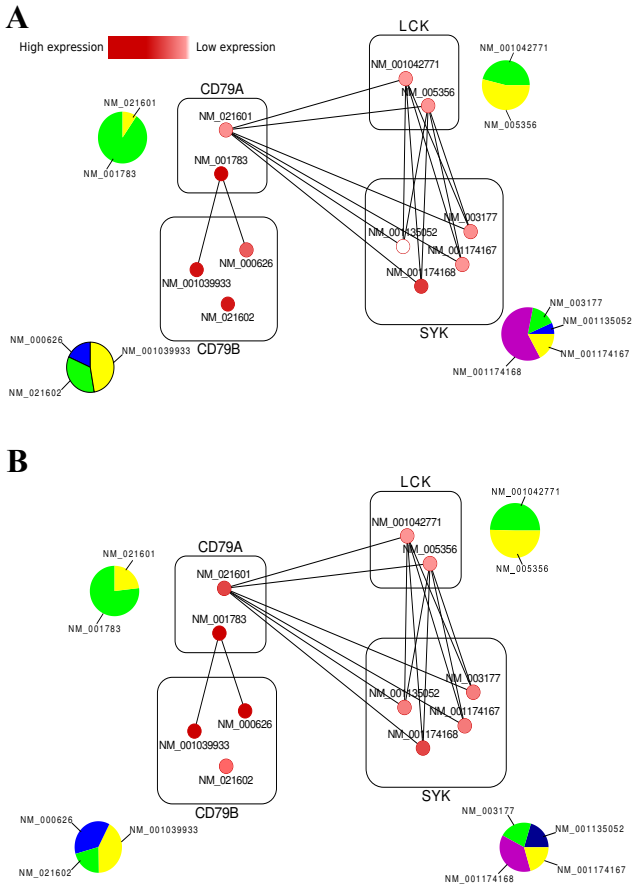

Figure 9. Transcript expressions estimated without or with transcript network. The transcript relative abundances (pie charts) and expressions (node rednesses) estimated on the four cancer genes described in Figure 1 for BRCA patient TCGA-A2-A04P are shown for (A) the EM algorithm (equation (**1**)) and (B) Net-RSTQ with protein domain-domain interactions.

smoothed to differentially expressed. (3) A transcript becomes differentially expressed when its neighbors' proportion affected by their neighbors. In Figure 8(C), none of the transcripts in gene TSHR is differentially expressed in BRCA (survival) dataset. However, transcript NM_000369 is connected to several non-differentially expressed neighbors and thus its proportion is altered by its neighbors. The smoothness to the proportion of NM_000369 leads to a change of the proportion of NM_001018036, which does not share any neighbor with NM_000369. In the end, NM_001018036 passively becomes differentially expressed. Note that these observed patterns do not necessarily improve the accuracy of differential transcript identification but the examples illustrate how the neighborhood in a transcript network plays a role in differential transcript analysis.

To further demonstrate the role of the domain-domain interactions modeled by the transcript network on the transcript proportion estimation in each RNA-Seq sample, we show the transcript relative abundances and expressions estimated without or with the network information on one patient sample in Figure 9(A) and 9(B), respectively. The subnetwork is the same network in Figure 1. In the figure, the redness of each transcript denotes the expression levels shown in the color bar. The relative abundances of the transcripts in one gene are reported in one pie chart. NM_000626 in gene CD79B and NM_021601 in gene CD79A are assigned a relatively lower proportion by EM in Figure 9(A). Since NM_000626 in gene CD78B shares the same highly expressed neighbor NM_001783 with NM_001039933, the two transcripts are assigned more similar proportions in Figure 9(B) by Net-RSTQ. Similar change is also observed for transcript NM_021601 in gene CD79A, which has a highly expressed neighbor NM_001174168 in gene SYK.

CONCLUSION

Many methods were proposed for transcript quantification with RNA-Seq data in the past five years (21). In this paper, we propose Net-RSTQ, a network-based RNA-Seq transcript quantification model, which to our knowledge is the first model that directly incorporates protein domain-domain interaction information for transcript proportion estimation. The experiments clearly demonstrated that the transcript expressions estimated with a transcript network constructed from protein domain-domain interactions can improve the transcript quantification and is more informative for patient

sample classification. The prior knowledge in the network can potentially corrects biases in probabilistic modeling as well as the RNA-Seq data. Based on the results, we concluded that utilizing transcript network information by Net-RSTQ effectively improve transcript analysis in RNA-Seq data.

ACKNOWLEDGEMENTS

Funding: This work was supported by NSF grant III 1117153. The results are based upon data generated by The Cancer Genome Atlas established by the NCI and NHGRI. Information about TCGA and the investigators and institutions who constitute the TCGA research network can be found at `http://cancergenome.nih.gov`. The dbGaP accession number to the specific version of the TCGA dataset is phs000178.v8.p7.

Conflict of interest statement. None declared.

REFERENCES

1. Ali Mortazavi, Brian A Williams, Kenneth McCue, Lorian Schaeffer, and Barbara Wold. Mapping and quantifying mammalian transcriptomes by RNA-Seq. *Nat Meth*, 5(7):621–628, 2008.
2. Eric T. Wang, Rickard Sandberg, Shujun Luo, Irina Khrebtukova, Lu Zhang, Christine Mayr, Stephen F. Kingsmore, Gary P. Schroth, and Christopher B. Burge. Alternative isoform regulation in human tissue transcriptomes. *Nature*, 456(7221):470–476, 2008.
3. Jingyi J. Li, Ci-Ren Jiang, James B. Brown, Haiyan Huang, and Peter J. Bickel. Sparse linear modeling of next-generation mRNA sequencing (RNA-Seq) data for isoform discovery and abundance estimation. *Proceedings of the National Academy of Sciences*, 108(50):19867–19872, 2011.
4. Cole Trapnell, Brian A. Williams, Geo Pertea, Ali Mortazavi, Gordon Kwan, Marijke J. van Baren, Steven L. Salzberg, Barbara J. Wold, and Lior Pachter. Transcript assembly and quantification by RNA-Seq reveals unannotated transcripts and isoform switching during cell differentiation. *Nat Biotech*, 28(5):511–515, 2010.
5. Wenyuan Li, Shuli Kang, Chun-Chi Liu, Shihua Zhang, Yi Shi, Yan Liu, and Xianghong Jasmine Zhou. High-resolution functional annotation of human transcriptome: predicting isoform functions by a novel multiple instance-based label propagation method. *Nucleic Acids Research*, 2013.
6. Ei-Wen Yang, Thomas Girke, and Tao Jiang. Differential gene expression analysis using coexpression and rna-seq data. *Bioinformatics*, 2013.
7. Martin Sauvageau Loyal Goff John L Rinn Lior Pachter Cole Trapnell, David G Hendrickson. Differential analysis of gene regulation at transcript resolution with rna-seq. *Nature Biotechnology*, (1):4653, 2012.
8. Adam Roberts, Cole Trapnell, Julie Donaghey, John Rinn, and Lior Pachter. Improving RNA-Seq expression estimates by correcting for fragment bias. *Genome Biology*, 12(3):R22, 2011.
9. Bo Li, Victor Ruotti, Ron M. Stewart, James A. Thomson, and Colin N. Dewey. RNA-Seq gene expression estimation with read mapping uncertainty. *Bioinformatics*, 26(4):493–500, 2010.
10. Ernest Turro, Shu-Yi Su, Angela Goncalves, Lachlan Coin, Sylvia Richardson, and Alex Lewin. Haplotype and isoform specific expression estimation using multi-mapping RNA-seq reads. *Genome Biology*, 12(2):R13, 2011.
11. Yan Huang, Yin Hu, Corbin D. Jones, James N. MacLeod, Derek Y. Chiang, Yufeng Liu, Jan F. Prins, and Jinze Liu. A Robust Method for Transcript Quantification with RNA-Seq Data. *Journal of Computational Biology*, 20(3):167–187, 2013.
12. Hui Jiang and Wing Hung Wong. Statistical inferences for isoform expression in RNA-Seq. *Bioinformatics*, 25(8):1026–1032, 2009.
13. Kim D. Pruitt, Tatiana A. Tatusova, Garth R. Brown, and Donna R. Maglott. NCBI Reference Sequences (RefSeq): current status, new features and genome annotation policy. *Nucleic Acids Research*, 40(Database-Issue):130–135, 2012.
14. Marco Punta, Penny C. Coggill, Ruth Y. Eberhardt, Jaina Mistry, John G. Tate, Chris Boursnell, Ningze Pang, Kristoffer Forslund, Goran Ceric, Jody Clements, Andreas Heger, Liisa Holm, Erik L. L. Sonnhammer, Sean R. Eddy, Alex Bateman, and Robert D. Finn. The Pfam protein families database. *Nucleic Acids Research*, 40(Database-Issue):290–301, 2012.
15. Robert D. Finn, Mhairi Marshall, and Alex Bateman. iPfam: visualization of proteinprotein interactions in PDB at domain and amino acid resolutions. *Bioinformatics*, 21(3):410–412, 2005.
16. Amelie Stein, Arnaud Ceol, and Patrick Aloy. 3did: identification and classification of domain-based interactions of known three-dimensional structure. *Nucleic Acids Research*, 39(Database-Issue):718–723, 2011.
17. Helen M. Berman, John D. Westbrook, Zukang Feng, Gary Gilliland, T. N. Bhat, Helge Weissig, Ilya N. Shindyalov, and Philip E. Bourne. The Protein Data Bank. *Nucleic Acids Research*, 28(1):235–242, 2000.
18. Sailu Yellaboina, Asba Tasneem, Dmitri V. Zaykin, Balaji Raghavachari, and Raja Jothi. DOMINE: a comprehensive collection of known and predicted domain-domain interactions. *Nucleic Acids Research*, 39(Database-Issue):730–735, 2011.
19. T. S. Keshava Prasad, Renu Goel, Kumaran Kandasamy, Shivakumar Keerthikumar, Sameer Kumar, Suresh Mathivanan, Deepthi Telikicherla, Rajesh Raju, Beema Shafreen, Abhilash Venugopal, Lavanya Balakrishnan, Arivusudar Marimuthu, Sutopa Banerjee, Devi S. Somanathan, Aimy Sebastian, Sandhya Rani, Somak Ray, C. J. Harrys Kishore, Sashi Kanth, Mukhtar Ahmed, Manoj K. Kashyap, Riaz Mohmood, Y. L. Ramachandra, V. Krishna, B. Abdul Rahiman, S. Sujatha Mohan, Prathibha Ranganathan, Subhashri Ramabadran, Raghothama Chaerkady, and Akhilesh Pandey. Human Protein Reference Database–2009 update. *Nucleic Acids Research*, 37(Database-Issue):767–772, 2009.
20. P. Andrew Futreal, Lachlan Coin, Mhairi Marshall, Thomas Down, Timothy Hubbard, Richard Wooster, Nazneen Rahman, and Michael R. Stratton. A census of human cancer genes. *Nature Reviews Cancer*, 4(3):177–183, March 2004.
21. Lior Pachter. Models for transcript quantification from RNA-Seq. 2011.
22. Yi Xing, Tianwei Yu, Ying Nian N. Wu, Meenakshi Roy, Joseph Kim, and Christopher Lee. An expectation-maximization algorithm for probabilistic reconstructions of full-length isoforms from splice graphs. *Nucleic acids research*, 34(10):3150–3160, 2006.
23. Hugues Richard, Marcel H. Schulz, Marc Sultan, Asja Nrnberger, Sabine Schrinner, Daniela Balzereit, Emilie Dagand, Axel Rasche, Hans Lehrach, Martin Vingron, Stefan A. Haas, and Marie-Laure Yaspo. Prediction of alternative isoforms from exon expression levels in RNA-Seq experiments. *Nucleic Acids Research*, 38(10):e112, 2010.
24. Bo Li and Colin N. Dewey. RSEM: accurate transcript quantification from RNA-Seq data with or without a reference genome. *BMC Bioinformatics*, 12:323, 2011.
25. Yoshiaki Tanaka, Kun-Yong Kim, Mei Zhong, Xinghua Pan, Sherman Morton Weissman, and In-Hyun Park. Transcriptional regulation in pluripotent stem cells by methyl cpg-binding protein 2 (mecp2). *Human Molecular Genetics*, 23(4):1045–1055, 2014.
26. Cole Trapnell, Lior Pachter, and Steven L. Salzberg. Tophat: discovering splice junctions with rna-seq. *Bioinformatics*, 25(9):1105–1111, 2009.
27. Heng Li, Bob Handsaker, Alec Wysoker, Tim Fennell, Jue Ruan, Nils Homer, Gabor Marth, Goncalo Abecasis, Richard Durbin, and 1000 Genome Project Data Processing Subgroup. The sequence alignment/map format and samtools. *Bioinformatics*, 25(16):2078–2079, 2009.
28. S. Kullback and R. A. Leibler. On information and sufficiency. *Ann. Math. Statist.*, 22(1):79–86, 1951.
29. Vladimir N. Vapnik. *Statistical learning theory*. Wiley, 1 edition, 1998.

Network-based Transcript Quantification with RNA-Seq Data

Wei Zhang [1], **Kay Minn** [2], **Lilong Lin** [3], **Baolin Wu** [4], **Jeremy Chien** [2], **Hui Zheng** [3], **and Rui Kuang** [1,*]

[1]Department of Computer Science and Engineering, University of Minnesota Twin Cities, Minneapolis, MN 55455, USA, [2]Department of Cancer Biology, University of Kansas Medical Center, Kansas City, KS 66160, USA, [3]Key Laboratory of Regenerative Biology, South China Institute for Stem Cell Biology and Regenerative Medicine, Guangzhou Institutes of Biomedicine and Health, Chinese Academy of Sciences, Guangzhou 510530, China and [4]Division of Biostatistics, School of Public Health, University of Minnesota Twin Cities, Minneapolis, MN 55455, USA

arXiv:1403.5029v1 [cs.CE] 20 Mar 2014

SUPPLEMENTARY

qRT-PCR experiment on a stem cell line

Total RNA was extracted from human embryonic stem (ES) H9 cells by using TRIzol (Invitrogen) and 5 g RNA was used to synthesize complementary DNA with ReverTra Ace (Toyobo) and oligo-dT (Takara) according to the manufacturer's instructions. Transcript levels of genes were determined by using Premix Ex Taq (Takara) and analysed with a CFX-96 Real Time system (Bio-Rad).

The templates for different transcripts were generated with PCR by using the template primers (Table 4). After isolation and purification, the templates were used to generate the standard curves with qRT-PCR by using the qRT-PCR primers (Table 4) for different transcripts. The generated standard curves have coefficient of determination (R2) over 0.999. The qRT-PCR primers were then applied to determine the expression levels of different transcripts in H9 ES cells by calculating with the standard curves. The expressions were carried out in three independent replications and the standard deviations were provided after the average.

qRT-PCR experiment on an ovarian cancer cell line

Total RNA is isolated from untreated ovarian cancer cells using Trizol (Invitrogen). RNA was reverse transcribed using Superscript II reverse transcriptase (Invitrogen) according to manufacture protocol. Real-time PCR was performed on CFX384 Real-time system (Bio-Rad) with FastStart SYBR Green Master (Roche) with the primer sets (Table 5). PCR conditions are 10 min at 95°C and 40 cycles of 95°C for 45 sec and 60°C for 45 sec.

Gene Name	Transcript Name	Estimated Proportion			qRT-PCR Results
		Net-RSTQ	EM	Cufflinks	
ABL1	NM_007313	64.46%	94.45%	71.07%	56±4.4%
	NM_005157	35.54%	5.55%	28.93%	44±4.4%
CBLC	NM_012116	73.12%	93.23%	87.59%	51±9.8%
	NM_001130852	26.88%	6.77%	12.41%	49±9.8%
KDM5C	NM_004187	80.52%	99.22%	100%	86±4.5%
	NM_001146702	19.48%	0.78%	0%	14±4.5%
KRAS	NM_033360	51.36%	80.23%	58.82%	36±4.2%
	NM_004985	48.64%	19.77%	41.18%	64±4.2%
NPM1	NM_002520	34.92%	55.84%	0%	52±10%
	NM_001037738	35.99%	37.60%	48.77%	3.2±10%
	NM_199185	29.09%	6.56%	51.23%	45±10%
TCF3	NM_003200	78.31%	98.11%	100%	56±6.5%
	NM_001136139	21.69%	1.89%	0%	44±6.5%
WHSC1L1	NM_023034	39.98%	73.61%	0%	46±6.1%
	NM_017778	60.02%	26.39%	100%	54±6.1%

Table 1. qRT-PCR results on H9 stem cell line.

Gene Name	Transcript Name	Estimated Proportion			qRT-PCR Results
		Net-RSTQ	EM	Cufflinks	
HNRNPA2B1	NM_031243	60.07%	81.42%	0%	82.83%
	NM_002137	39.93%	18.58%	100%	17.17%
HRAS	NM_176795	36.19%	98.35%	36.92%	50.16%
	NM_001130442	34.11%	1.65%	0%	NA
	NM_005343	29.7%	0%	63.08%	49.84%
NSD1	NM_022455	55.4%	96.39%	100%	99.98%
	NM_172349	44.6%	3.61%	0%	0.02%
TSC2	NM_000548	35.06%	69.47%	0%	45.36%
	NM_001077183	31.86%	5.75%	100%	54.64%
	NM_001114382	33.08%	24.78%	0%	NA
WHSC1L1	NM_023034	48.84%	63.85%	0%	18.81%
	NM_017778	51.16%	36.15%	100%	81.19%

Table 2. qRT-PCR results on OVCAR8 cancer cell line.

*To whom correspondence should be addressed. Tel: +1 612 6247820; Fax: +1 612 6250572; Email: kuang@cs.umn.edu

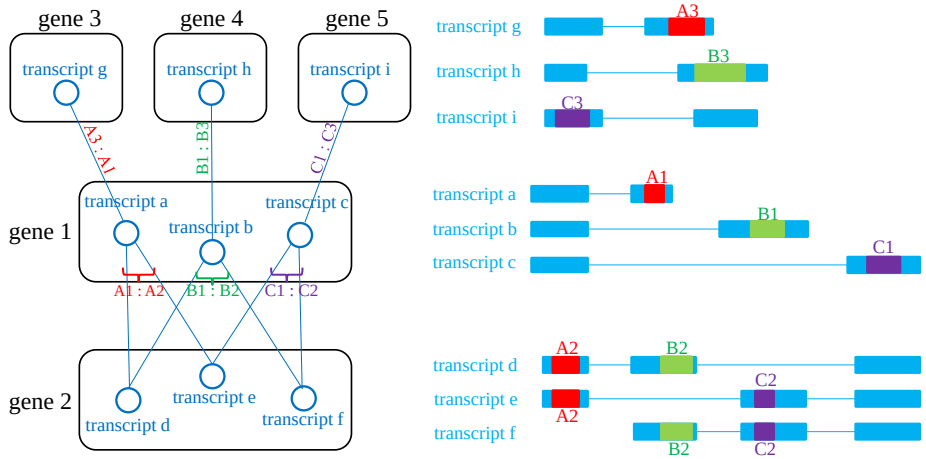

Figure 1. A simulated example of transcript network based on protein domain-domain interactions. In this example, nine transcripts in five genes are considered. The exons and domain annotations are shown in the right figure. The domains in the same color, {A1,A2,A3}, {B1,B2,B3} and {C1,C2,C3} interact with each other. In the network on the left, the transcripts are connected if they contain a pair of interaction domains. For example, the three transcripts a, b and c are connected with different transcripts/genes by domain-domain interactions (annotated on each edge).

Dataset	OV(Survival)	OV(Relapse)	BRCA(Survival)	BRCA(Relapse)	LUAD(Survival)	LUSC(Survival)
Net-RSTQ	0.5973	0.6070	0.6826	0.5902	0.6353	0.5666
Net-RSTQ (remove negative CC)	0.5950	0.6098	0.6796	0.5876	0.6340	0.5685
# of removed interactions with CC<-0.1 (%)	274 (2.25%)	256 (2.11%)	948 (7.80%)	1254 (10.32%)	506 (4.16%)	253 (2.08%)

Table 3. Comparison of classification performance using transcript networks with or without negative correlations. Classification results of estimated transcript expressions by Net-RSTQ with (first row) and without (second row) interactions between negatively correlated transcripts. The number of removed interactions with correlation coefficients (CC) less than -0.1 in each dataset is reported in the third row. The mean AUC scores of classifying patients by the estimated transcript expression for each dataset are reported.

Gene/Transcript(isoform) Names	Primer Names*	Forward	Reverse
ABL1	Template 1&2	5-GGTTGGTGACTTCCACAGGAAA	5-CACCGTCAGGCTGTATTTCTTCC
NM_007313(iso2)	qPCR 1&2	5-TGAAAAGCTCCGGGTCTTAGG	5-TTGACTGGCGTGATGTAGTTG
NM_005157(iso1)	qPCR 2	5-TAGCCAAAGACCATCAGCGTT	5-TTCGCGGTTATCAATTTCATGT
CBCL	Template 1&2	5-ACCCTGTGGAACCAGGCTGC	5-CACCTGCCCCAGCTCCAACT
NM_012116(iso1)	qPCR 1&2	5-ACCACCATTGACCTCACCTGC	5-ACTGCCAGGAGCTGCCAGTT
NM_001130852(iso2)	qPCR 1	5-CATCCTGCAGACCATCCCTG	5-GGCCGAGCTCAGTCAGGTCT
KDM5C	Template 1&2	5-GACCTGCTCGAGGTGACCCT	5-AAGCTTTCTTCAGATCACAGGGAG
NM_004187(iso1)	qPCR 1&2	5-GCCTCTAACCAGCATTCCCA	5-TCTCTGGAATGGTGATGGCC
NM_001146702(iso2)	qPCR 1	5-AGAGGCTGAGGAGGTCCAGG	5-CCAAGCCATTCTGGTTCTCC
TCF3	Template 1&2	5-TGAATCCCAAAGCAGCCTG	5-TCTTGTAACTAATGTTTTTATTTTCCTTA
NM_003200(iso1)	qPCR 1&2	5-TGAATCCCAAAGCAGCCTGT	5-GGTTGTGGGCTTCGCTCAG
NM_001136139(iso2)	qPCR 1	5-GTATGCCTCCGTGGGACGA	5-GGAGCTCCTGGACCCAGTGT
WHSC1L1	Template 1	5-CAGTTCCTCAGGCTACAGTGAAGA	5-CATACAACAAACAGACATCTAGATCAAC
NM_023034(iso1)	Template 2	5-CAGTTCCTCAGGCTACAGTGAAGA	5-GTAATGTAGTTTCTTGCCAGCTTTACA
NM_017778(iso2)	qPCR 1	5-GTCGGCGGCTTGATAAACAGT	5-GTACCCATCCAGCTCAAACCG
	qPCR 2	5- CCCTTCAGCTACTGCAGATGC	5-CCAGGCACTCCAGGTGAAAGT
KRAS	Template 1	5-TTCCTGCTCCATGCAGACTGT	5-TAAGAAGTAATCAACTGCATGCACCA
NM_033360(iso2)	Template 2	5-TACATTGGTGAGGGAGATCCGA	5-TAAGAAGTAATCAACTGCATGCACCA
NM_004985(iso1)	qPCR 1	5-TTCCTGCTCCATGCAGACTGT	5-GCACCAAAAACCCCAAGACAG
	qPCR 2	5- TACATTGGTGAGGGAGATCCGA	5-TAGAAGGCATCATCAACACCCA
NMP1	Template 1&2&3	5-TCCTTTCCCTGGTGTGATTCC	5-CATTGTCAGGTGAGGCAAATGC
NM_002520(iso1)	qPCR 1&2&3	5-TCCTTTCCCTGGTGTGATTCC	5-TCGGCCTTTAGTTCACAACCG
NM_0010337738(iso3)	qPCR 1&3	5-AGCTGAAGAAAAAGCGCCAGT	5-CTTTTGTGCATTTTTGGCTGG
NM_199185(iso2)	qPCR 3	5-AAGCCCAAAGATGGGGAGAA	5-AAGGGCAAGGTTCACTGAATCA

Table 4. Primer sets of the transcripts in seven genes of H9 stem cell line. * The numbers refer to the isoforms in the first column.

Gene Name	Transcript Name	Primer Sequence - Forward	Primer Sequence - Reverse
HNRNPA2B1	NM_031243	TCC GCG ATG GAG GAA AAC TTT AG	GCC ACC AAT AAA GAG CTT ACG G
	NM_002137	AGC GGC AGT TCT CAC TAC AG	TCC TTT TCT CTC CTC CAT CG
HRAS	NM_176795	CCG CTC TGG CTC TAG CTC	ACC AAC GTG TAG AAG GCA TCC
	NM_005343	AGG ATG CCT TCT ACA CGT TGG	CAT GTC CTG AGC TTG TGC CT
NSD-1	NM_022455	TCG CCA TTC TTG CCA TTA GC	TTT TCA TTG CTG CCG TCC AC
	NM_172349	ATT GTC TGC TGC CCT TTT CC	TGG AAT CTG GAT CAT CCC GA
TSC2	NM_000548	CTC TCC ACC CGT GAA AGA ATT C	GAC CAC ATG TTC AGA CAC ACT G
	NM_001077183	AAC GAG AGA CCC AAG AGG AT	GA CGT ATC GAG CCA TCA TGT C
WHSC1L1	NM_023034	ATG TAA AAC TGG GGC AGC AC	AAG CAC CAA CAG AAC AAC GC
	NM_017778	TTT CGG TTT GAG CTG GAT GG	TTT GGG CTG TTT GGC AAA CC

Table 5. Primer sets of the transcripts in five genes of OVCAR8 cancer cell line.